The Bell System Technical Journal
Vol. 55, No. 10, December 1976
Printed in U.S.A.

Novel Technique for Measuring the Index Profile of Optical Fibers

By J. A. ARNAUD and R. M. DEROSIER

(Manuscript received August 30, 1976)

A novel technique for measuring the refractive index profile of optical fibers is demonstrated, which offers substantial advantages over alternative methods. The method consists of illuminating a small area of the fiber core and measuring the total transmitted power. The transmission of leaky modes is accounted for in the manner reported previously by other authors. The index profiles of germanium-doped fibers obtained by this technique are compared to interferometric measurements. The resolution is shown to be limited by wave optics effects to about $\lambda_o(4n\sqrt{2\Delta})^{-1}$, *where* $\Delta \equiv \Delta n/n$. *The distortion of the index profile as the wavelength varies and wave-optics effects are investigated.*

I. INTRODUCTION

The accurate measurement of index profiles at various wavelengths may help design multimode fibers whose transmission capacity would go well beyond what has been presently achieved. Indeed, numerical calculations and theoretical analyses[1,2] show that there exist index profiles (usually not power-law profiles), which, for quasi-monochromatic sources, provide transmission capacities of about $1.6/\Delta^2$ Mb/s × km, where $\Delta \equiv \Delta n/n$. Measured transmission capacities are about 10 times smaller. To determine the optimum profiles, it is indispensable to know the variation of $dn/d\lambda_o$ (where λ_o is the operating wavelength) as a function of n for the class of materials considered with an accuracy of about 1 percent. The required variation of $dn/d\lambda_o$ as a function of n can be obtained, in principle, from measurements on bulk samples (e.g., Ref. 3). We question, however, whether measurements on bulk samples are applicable to the fiber material with sufficient accuracy. For that reason and also because the fabrication and measurement of bulk samples is time-consuming, the direct measurement of index profiles at various wavelengths is highly desirable. Once the optimum profile applicable to the class of materials considered has been determined, we measure the departures of the profile $n(r)$ of the fabricated

fiber from optimum. Very small deviations may degrade considerably the transmission capacity.

An interesting experimental technique for measuring circularly symmetric index profiles has heen proposed hy Gloge and Marcatili.[4] The index profile is obtained hy measuring with a pin hole the radial distrihution of intensity in fibers excited hy Lambertian (e.g., thermal) sources. In a series of careful measurements, Sladen, Payne, and Adams[5] have shown that good agreement can he ohtained hetween the intensity in the fiher core and the index profile obtained by interferometry provided the non-zero transmission of the leaky modes is accounted for. If this correction is made, the fiher samples need not he larger than ahout 1 meter, and may be as small as 1 cm.

The technique that we describe in the present paper, which we call the transmission technique, is related to the near-field technique discussed ahove, but it differs from it in many significant ways. Arnaud[6] has shown that, if we illuminate a small area of the fiher core (perhaps of the order of $(\lambda_o^2$ at x, y, the total transmitted power is, for sufficiently long fihers, proportional to $n^2(x, y) - n_c^2$, where $n(x, y)$ denotes the refractive index at x, y, and n_c, the cladding index. The proof is straightforward: The rays radiated from the illuminated area have an almost uniform distrihution in the plane k_x, k_y, where k_x, k_y denote the transverse components of the wave vector $\mathbf{k}$. Because of the relation $k_x^2 + k_y^2 + k_z^2 = k^2(x, y) \equiv (\omega/c)^2 n^2(x, y)$, which holds hetween the rectangular components of $\mathbf{k}$, and hecause only rays whose k_z is larger than k_s are transmitted without loss, the power transmitted through long fihers is proportional to

$$k_x^2 + k_y^2 = k^2(x, y) - k_s^2 \equiv \text{index profile} \tag{1}$$

(see Fig. 1). The rays in the dotted area in Fig. 1b leak away if the fiher is sufficiently long. Otherwise their contrihution to the total transmitted power needs to be suhtracted in the manner reported in Ref. 5. If the spot size is less than λ_o, we may use as a source either a (coherent) laser or a (spatially incoherent) LED. If, however, the spot size is significantly larger than λ_o, it is essential to use near-Lambertian sources such as LEDs. Indeed, coherent beams of large cross section would excite predominantly paraxial rays. This would require introducing additional correction factors.

In the present paper, we discuss the principles and limitations of the method, and we present experimental results. The transmission method gives results that are, in principle, identical to the near-field measurements described in Ref. 5. The main advantage of the transmission method, compared with alternative methods, including the near-field technique, is that it is extremely easy to implement. The results are highly reproducible to better than one part in 1000.

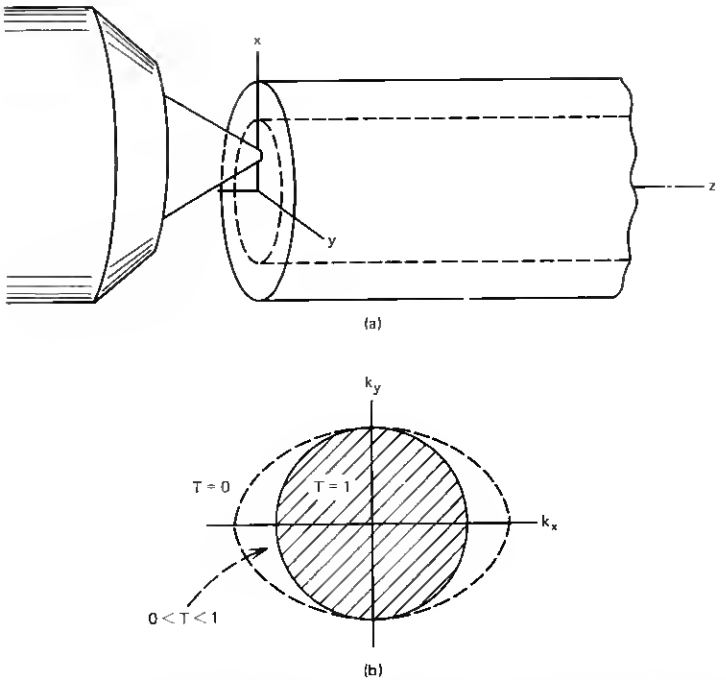

Fig. 1—(a) In the transmission method, the microscope objective illuminates a small area of the fiber end of the order of λ_0^2. (b) The intensity is assumed uniform in the k_x, k_y space. For long fibers, only the rays in the shaded area are transmitted. For short fibers, the rays in the dotted area may also be transmitted (leaky rays). T denotes the power transmission.

II. EXPERIMENTAL CONDITIONS

To implement the proposed technique, all we need is an ordinary microscope, a high-radiance LED (or a laser), and a detector. The numerical aperture (NA) of the microscope objective should be at least twice as large as that of the fiber. One end of the fiber is properly broken or polished and centered approximately under the microscope objective at focus. When the microscope eyepiece is replaced by a LED, a small spot of infrared radiation illuminates the fiber end. As we have indicated in the introduction, the power detected at the other end of the fiber is proportional to $n^2(x, y) - n_c^2$, where $n(x, y)$ denotes the index at the point x, y of the fiber where the light is focused, and n_c the cladding index. To obtain the index profile, we may scan either the fiber, with a total motion of about 100 μm, or the source, with a total motion of about 3 mm. The arrangement shown in Fig. 2 incorporates a beam splitter (1) to allow the fiber to be observed during scanning. (A second beam splitter, which combines the light from two LEDs, is shown in Fig. 2. It is used only for dispersion measurements.) Some infrared LEDs radiate red light with sufficient intensity for direct visual

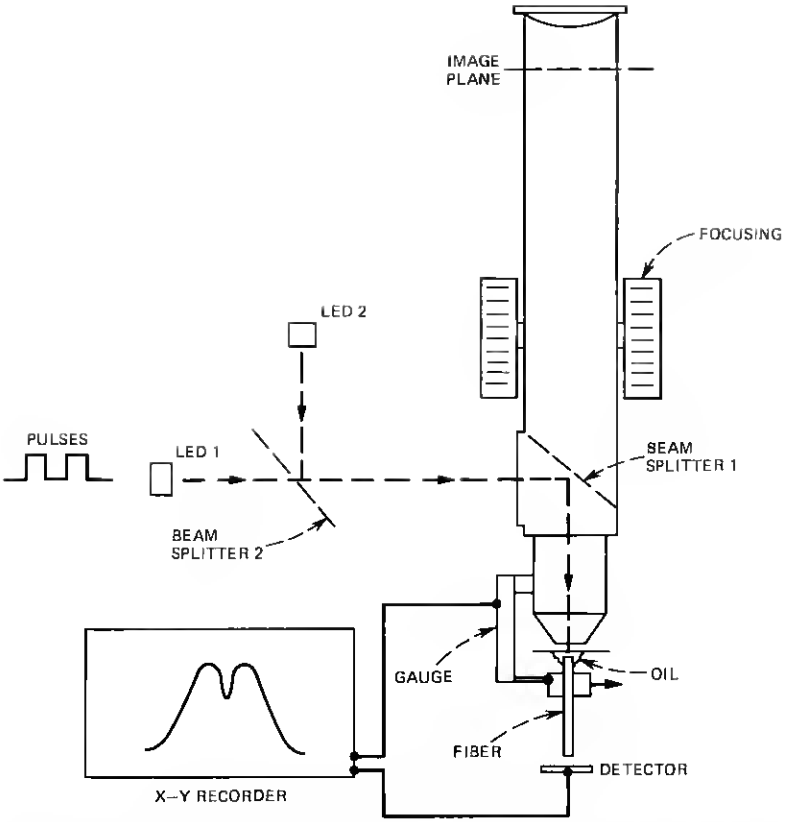

Fig. 2—Experimental setup of the transmission technique. The fiber is scanned mechanically and its motion is recorded with a gauge. Two LEDs are used for dispersion measurement.

observation. For LEDs at longer wavelengths, an image converter is necessary. Note that the focal length of microscope objectives may be slightly different for the red light and for the infrared light. In the arrangement in Fig. 2, it is convenient to have the distance between the LED source and the microscope objective equal to the distance between the focal plane of the eyepiece and the microscope objective. This avoids the need for refocusing when the objective is changed from low to high magnification. To obtain good resolution, it is desirable that the LED act as a point source; that is, that the apparent size of the LED, demagnified by the microscope objective, be smaller than the diffraction-limited spot $\approx\lambda_o/\mathrm{NA}$, defined by the numerical aperture of the microscope objective. An apparent emissive diameter of 25 μm (before demagnification) is adequate. The experimental setup is shown in Fig. 3. The LED source (not visible) is supported by the

xyz microscope stage at the left. The angular orientation of the fiber under the microscope objective can be varied. Figure 3 shows the differential micrometer that drives the fiber and the gauge that measures its displacement with respect to the microscope objective.

The advantages of the proposed technique compared to the more conventional near-field technique are many:

(*i*) In the near-field method, the source is required to be Lambertian and uniform over the full cross section of the fiber core. As pointed out in Ref. 5, this condition is in fact difficult to

Fig. 3—Photograph of the experimental setup. The LED (not seen) is supported by the xyz stage on the left.

achieve with LEDs. The authors in Ref. 5 thus found it necessary to use thermal sources instead of LEDs. Thermal sources (e.g., tungsten wires) provide poor signal-to-noise ratios when the spectral width is restricted hy narrowband interference filters. In the transmission method, we require the NA of the microscope ohjective to he significantly larger than that of the fiher (at least for coherent sources), hut the requirement concerning the spatial uniformity of the source is relaxed. In some sense, the requirement of spatial uniformity is transferred from the source, where it is difficult to achieve, to the detector, where the condition is easily met.

(*ii*) The optics are much simplified. Only a single microscope ohjective is needed instead of (typically) three. Thus, the signal-to-noise ratio is improved.

(*iii*) Near-field measurements provide the shape of the index profile, hut not the absolute value of $\Delta n(r) = n(r) - n_c$, where n_c denotes the cladding index. In the transmission method, we can calihrate Δn hy measuring the intensity radiated axially hy the microscope ohjective. This calihration technique will he discussed in more detail in the next section.

(*iv*) The transmission method can he comhined with the Fresnel-reflection technique (for a recent report of the Fresnel-reflection technique, see Ref. 7). To implement this modification, we replace the microscope eyepiece in Fig. 2 with a detector.

An important drawhack that applies to both the transmission and near-field methods is encountered when the fiher exhihits a low-index region near the cladding. In that case, some modes (hesides the so-called weakly leaky modes) are leaking very slowly, and the interpretation of the measurements hecomes amhiguous. The resolution offered hy these methods may he marginal when the fiher profile exhihits very fast fluctuations. Note also that, for noncircularly symmetric profiles, the correction factors for leaky rays have not heen worked out. If the deviation from perfect circular symmetry is small, however, the correction factor given in Ref. 5 may be used.

III. INCIDENT BEAM PATTERN AND INDEX CALIBRATION

To make precise measurements, the radiation from the microscope ohjective should approximately ohey Lamhert's law, at least for angles α to the axis that are less than $\sqrt{2\Delta}$. To verify that this law is approximately oheyed, we translate the detector in front of the microscope ohjective at some distance $d \gg \lambda_o$ from the focal point. Ideally, the variation of the detected power as a function of the distance r from

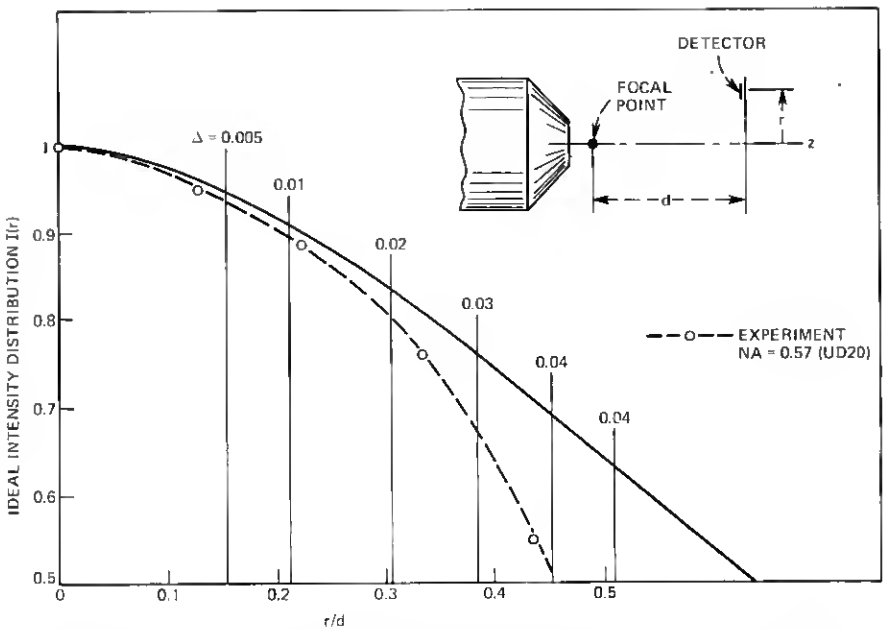

Fig. 4—The curve shown is the desired radiation pattern from the microscope objective. It is sufficient if this law be obeyed from $r/d = 0$ to the value corresponding to the Δ of the fiber (e.g., $r/d < 0.3$ if $\Delta = 0.02$). The experimental points were measured using a Leitz UD 20, NA = 0.57 microscope objective.

axis should be*

$$P(r) = \cos^4 \alpha = (1 + r^2/d^2)^{-2}. \tag{2}$$

The desired variation of P with r in (2) is shown in Fig. 4. The maximum value of r/d corresponding to a particular Δ is given by

$$r/d = (\text{NA}^{-1} - 1)^{-\frac{1}{2}} \tag{3a}$$

$$\text{NA} = n_o\sqrt{2\Delta}. \tag{3b}$$

The values of r/d are shown in Fig. 4 for typical values of Δ and $n_o = 1.45$.

Let us now consider the prohlem of calibrating Δn. This is done by measuring the intensity radiated axially hy the microscope ohjective.

* This result can be obtained by inverting eq. (5.246) of Ref. 6 and noticing that when the radiation is uniformly dense in the k_x, k_y plane (the transverse components of the wave vector), it remains uniformly dense after refraction at any plane interface perpendicular to the z axis. To show that, set in eq. (4.167) of Ref. 6: $dk_x/dz = dk_y/dz = 0$ (Descartes-Snell law) and find that $f(k_x, k_y, x, z) = g(k_x, k_y)h(x, z)$ is a solution of the Liouville equation for any differentiable functions g and h. Thus, if f is independent of k_x and k_y at $z = 0$, as we have assumed (Lambert's law), it remains independent at k_x, k_y after any number of refractions.

Let the power detected in front of the microscope objective be denoted P_c and tbe power transmitted through the fiber for near-axial excitation be denoted P. If the detector radius is denoted ρ and its distance from tbe microscope objective focal point is d, the NA $= n_o\sqrt{2\Delta}$ of tbe fiber is given by

$$\text{NA} = (\rho/d)\sqrt{P/\eta P_c}, \tag{4}$$

wbere

$$\eta = [4n_o/(n_o + 1)^2]^2 \tag{5}$$

accounts for tbe Fresnel reflection at botb ends of tbe fiber. Tbis expression for η is not rigorous, hut it is sufficiently accurate for our application. Witb sufficient accuracy, we can set $n_o = 1.45$. Tben, $\eta = 0.93$. Convenient values for d and ρ are $d = 10$ mm and $\rho = 1$ mm, respectivcly. We thus obtain from (4) and (5)

$$\text{NA} = 0.104\sqrt{P/P_c} \tag{6a}$$

$$\Delta = 0.00255(P/P_c). \tag{6b}$$

It is, of course, necessary to bave good hreaks at botb ends of the fiber. We bave assumed that the fiber loss is ncgligible; tbis is tbe case for most fihers if the lengtb is 1 m or less.*

A more conventional tecbnique for evaluating Δ consists of measuring tbe far-field pattern wben tbe fiber is illuminated on or near axis. We bave

$$\Delta = \tfrac{1}{2}(\text{NA}/n_o)^2, \tag{7}$$

where NA denotes the sinus of the maximum radiation angle in air, defined typically at the -3 dB point from maximum intensity.

Tbe core radius, a, of the fiber is best obtained by observing tbe fiber tip witb a microscope. From the values of Δ, a, and λ_o, tbe V-number is calculated according to

$$V = (2\pi a/\lambda_o)\text{NA}. \tag{8}$$

IV. CORRECTION FOR LEAKY RAYS

If the fiher is not very long, the leaky modes excited by tbe source are not completely attenuated. They can he accounted for in tbe manner described in Ref. 5. Specifically, the index profile $n^2(r) - n_c^2$ is obtained by dividing the detected power $P(r)$ by tbe correction factor

* With some high NA objectives (NA ≈ 0.8), spurious peaks are observed in the far-field pattern due to diffraction effects, even with LED sources. Thus, the calihration of Δ should he made with lower NA objectives, e.g., NA ≈ 0.5. These spurious peaks do not appear to affect the profile measurements, hut they prevented us from making a precise comparison hetween the two techniques described here for measuring Δ.

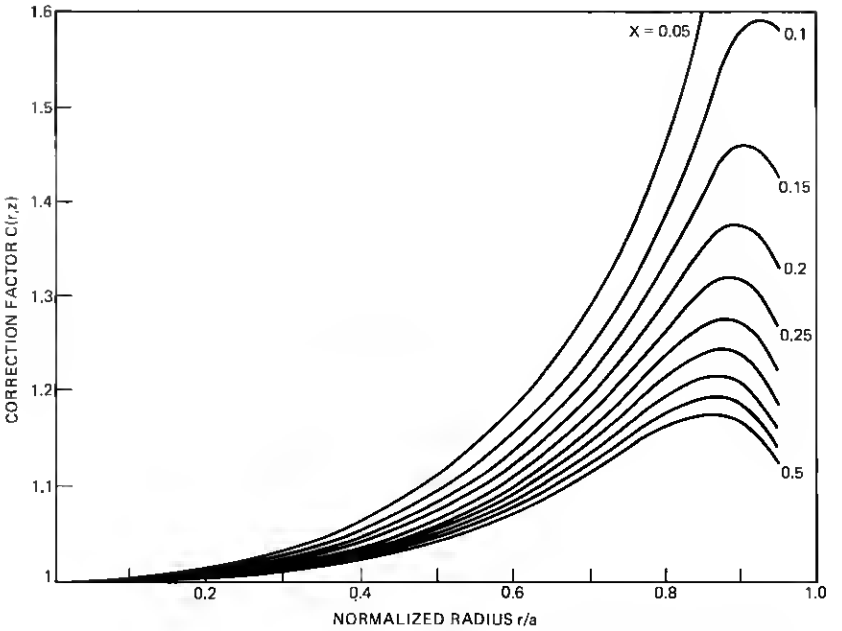

Fig. 5—Correction factor for leaky rays.[6] The X parameter is defined in the main text as $X = V^{-1} \log_e(L/a)$, where V denotes the V-number of the fiber, L, the fiber length, and a, the core radius. The measured power should be divided by C. These curves are applicable to near-square-law fibers.

$C(r)$ given in Fig. 5.[5] In this figure, the parameter X is defined as

$$X = V^{-1} \log_e(L/a), \tag{9}$$

where L denotes the fiber length, and V the fiber V-number defined in (8).

Note that the correction is negligible near the fiber axis, but may be as large as 30 percent at $r \approx 0.8a$ for typical fiber lengths. Strictly speaking, the correction factor depends on the profile of the fiber. The curves in Fig. 5 are applicable to near square-law profiles. However, the correction factor turns out not to be very sensitive to the exact profile. Thus, for most high-transmission capacity fibers, the square-law-profile correction factor may be sufficiently accurate. If greater accuracy is required, we may use an iteration procedure. Because this procedure is rather involved, it will not be discussed here.

V. REFRACTIVE-INDEX PROFILE MEASUREMENTS

The measurement technique described in previous sections has been applied to graded-index fibers. Let us first make a few general comments concerning the experimental technique and the results. The

results obtained are highly reproducible to hetter than one part in 1000 even after a few hours if the fiher tip is protected hy a glass plate and an index-matching fluid. The axial index dip characteristic of germanium- (or phosphor-oxide-) doped fihers is very useful to define the fiher center and achieve optimum focusing.

5.1 Comparison with near-field and interferometric measurements

Near-field measurements[5] were made on a graded-index fiher. The setup is shown schematically in Fig. 6a. A Burrus-type high-radiance LED with an apparent emissive diameter of 50 μm is imaged with unity magnification on the end of the fiber under test with a pair of microscope ohjectives (20×, NA = 0.4). The other end of the fiher is imaged with a microscope ohjective (40×, NA = 0.65) on a scanned small-area detector. The magnification, measured with a reticle, is equal to 54. Focusing is adjusted to make the details of the index profile as sharp as possihle. The variation of detected power as a function of the transverse displacement of the detector is shown in

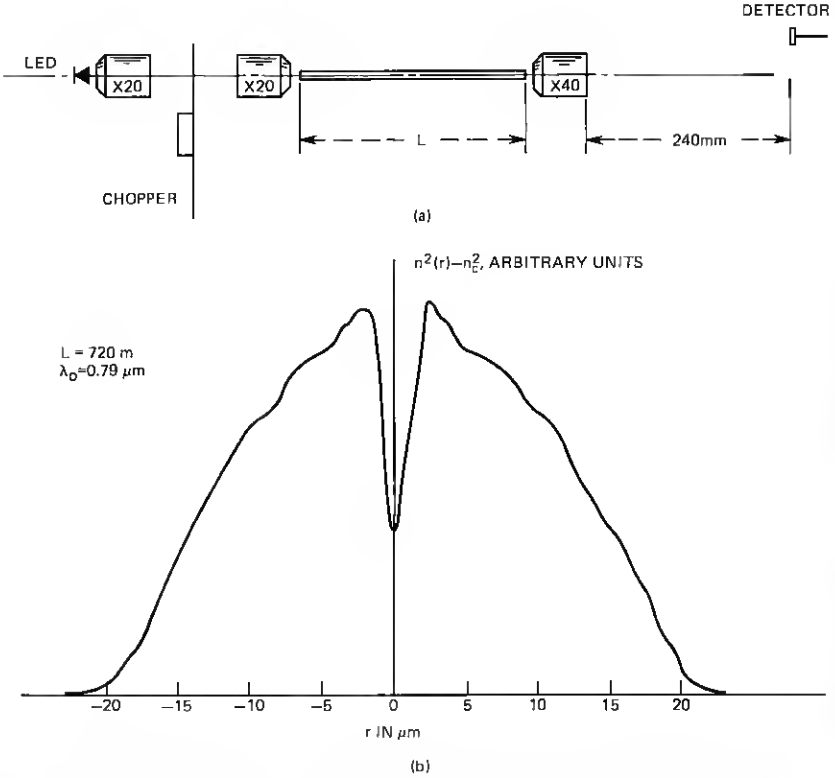

Fig. 6—Near-field measurement on a germanium-doped, graded-index fiber.

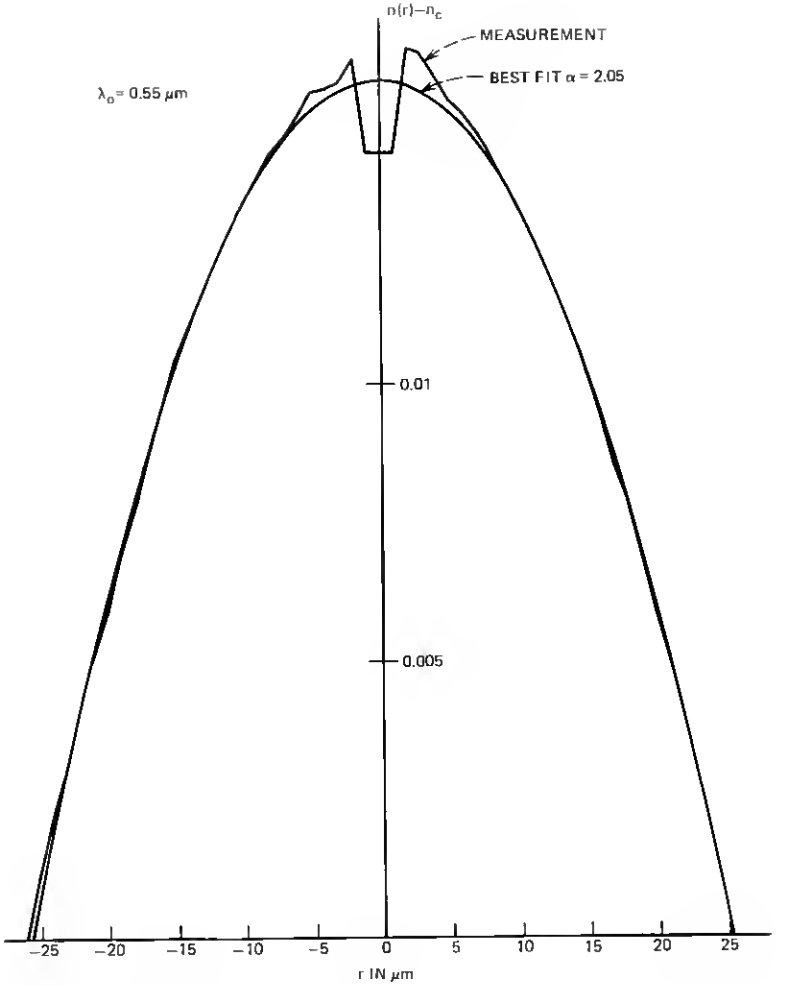

Fig. 7—Interferometric profile of the fiber in Fig. 6, $\lambda_0 = 0.55$ μm. NA = 0.21, $\Delta = 0.0107$.[8]

Fig. 6h for a fiber length $L = 720$ m. For such long lengths, the leaky-ray correction is small. Because of evaporation of germanium during the collapse of the preform, the material on axis is probably almost pure silica. The observed reduction of Δn is, at most, $\frac{2}{3}$. This discrepancy reflects the inherent limitation in resolution of near-field and transmission techniques. We attribute small oscillations on each sides of the central dip to wave-optics effects. They are qualitatively similar to the ones calculated for a dielectric slab in Appendix A. The slow modulation reflects the presence of diffused steps. The interferometric measurement[8] is shown in Fig. 7.

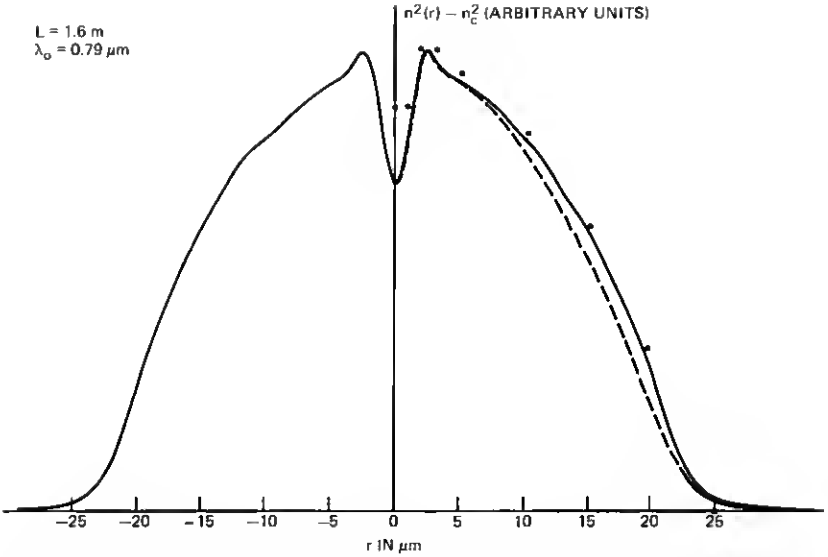

Fig. 8—Profile of the fiber in Figs. 6 and 7 obtained with the transmission technique. Uncorrected: solid line. Corrected for leaky rays: dashed line. Interferometric measurements from Fig. 7: dots. The measured Δ at $\lambda_0 = 0.79$ μm is 0.0104.

The index profile ohtained with our transmission technique is shown in Fig. 8. The Δ of the fiher was measured from the far-field pattern, as described in Section III. We measured $\Delta = 0.0104$, in good agreement with the value ohtained by interferometry. From a core radius $a = 24$ μm, we calculate from (8) a V-numher: $V = 40$. The fiher length is 1.6 m. Thus, the X-parameter in (9) is $X = 0.28$. The corrected profile, ohtained hy dividing the measured power hy the correction factor C in Fig. 5, is shown as a dashed line in Fig. 8. The result of interferometric measurements is shown hy dots for comparison. Aside from the depth of the central dip, a significant difference hetween the dashed curve (corrected transmission profile) and the dots (interferometric measurement). Such a discrepancy may be in part attrihuted to the lack of perfect circular symmetry of the fiher.

5.2 *Measurement of the lack of circuler symmetry*

The (uncorrected) transmission profile of germanium-doped fiher was measured in two perpendicular azimuthal directions, laheled 0° and 90°, respectively. These two profiles are shown in Fig. 9 as solid lines and dashed lines, respectively. The measured Δ and NA parameters are given in the figure caption. We conjecture that, for the small deviations from circular symmetry exhibited by the fiher investigated, the correction factor in Fig. 5 is applicable.

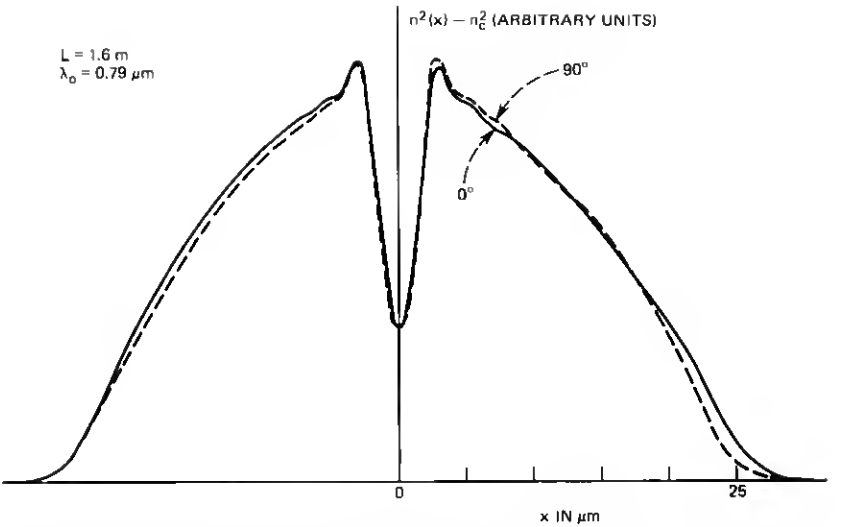

Fig. 9—Uncorrected profile of a germanium-doped, graded-index fiber in two azimuthal planes (0° and 90°). The measured NA is 0.202, $\Delta = 0.00974$, $L = 1.6$ m.

5.3 Measurement of a double-hump profile fiber

An attempt was made by MacChesney[9] to suppress the central index dip of germanium-doped fibers by increasing the amount of germanium halides during the final stage of fabrication of the preform. The profile of a fiber of that type was measured by interferometry[8] and by our transmission technique. Both techniques clearly show that there is a large *peak* of index near the center of the fiber. However, the transmission technique shows that the dip in the center did not disappear (hence, the name "double-hump" given to the profile of that fiber). This central dip is not seen on the interferogram. The combination of a peak and a dip is unlikely to improve the fiber transmission. A much better compensation of the central dip will be reported later in this paper.

5.4 Measurement of noncircularly symmetric profiles

The theoretical result in (1) shows that the transmission technique is applicable, in principle, to noncircularly symmetric profiles, as well as to circularly symmetric profiles. A preform that accidentally collapsed flat[10] has been pulled at our request into a fiber and measured. The uncorrected profiles are shown in Fig. 10. Because the correction for the leaky rays has not been made, the curves in Fig. 10 are only indicative of the index profile.

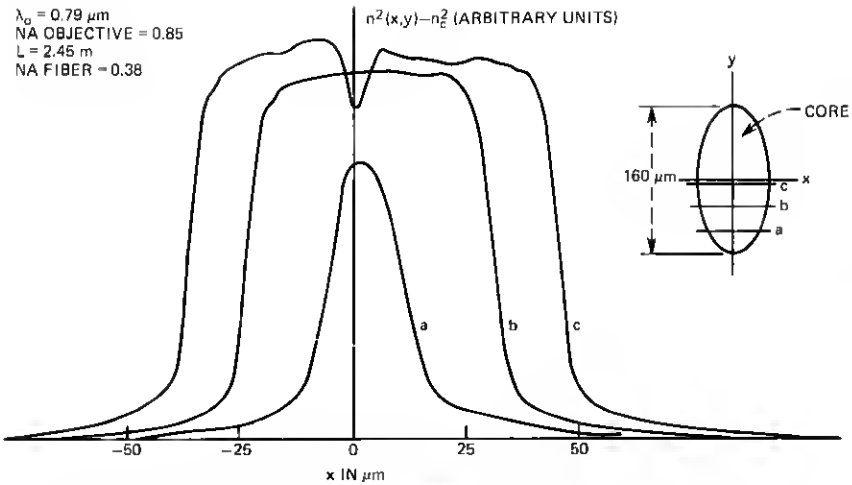

Fig. 10—Profile of a fiber with near-elliptical core (uncorrected).

5.5 Profile distortion

One of the most interesting and intriguing questions is whether index profiles get significantly distorted as the wavelength varies (independently of possihle changes of scale). Fleming's measurements on bulk samples of germanium-doped silica[3] clearly indicate that profiles get distorted significantly as the wavelength varies. This effect, however, has not heen ohserved hefore on fihers. We report here preliminary measurements of profile distortion. The necessary formulas are relegated to Appendix B.

Figure 11 shows the profiles measured with the transmission method at two wavelengths: $\lambda_o = 0.79$ μm and $\lambda_o = 0.9$ μm, on a germanium-doped, graded-index, large NA fiber. Note first that the resolution (indicated hy the depth of the central dip) is slightly poorer at the longer wavelength. When the scanning is made slightly off-center to avoid the central dip and the two profiles are normalized to unity on axis, the differences hetween the two profiles are found to he extremely small yet significant. To exhihit this difference with good accuracy, we have comhined the light from the two LEDs with heam splitter in Fig. 2 number 2. Square pulses are applied to the LEDs. The positive parts of the pulses drive one LED and the negative parts drive the other. The levels are adjusted to have equal detected powers on the fiber axis, and therefore, zero signal on the lock-in amplifier. The difference between the two normalized profiles is plotted in Fig. 12 (curve h). More precisely, we have plotted in Fig. 12 the "profile distortion" $d \equiv \lambda_o \partial\eta/\partial\lambda_o$, where $n \equiv N/2\Delta$ and $N \equiv 1 - n^2/n_o^2$, as a function of r/a. The accuracy of this curve is difficult to ascertain at

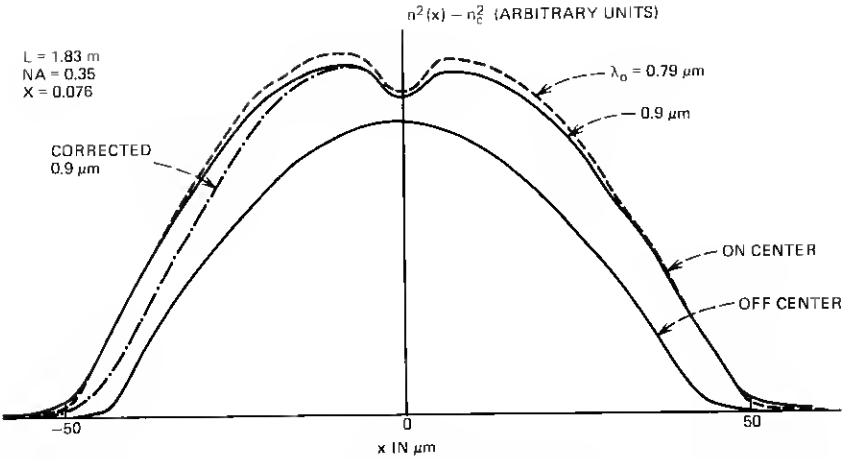

Fig. 11—Profile of a germanium-doped, graded-index fiber at two wavelengths (a): $\lambda_0 = 0.79$ μm, (b) $\lambda_0 = 0.9$ μm, (c) $\lambda_0 = 0.79$, scanning slightly off-center (obtained with the transmission technique and an objective NA = 0.85).

the moment. Part of the observed change of the shape of the index profile may be attributed to the dependence of the leaky-ray correction factor on wavelength.

The variation of d as a function of r/a can also be calculated from Fleming's measurements on bulk samples, as explained in detail in Appendix B. The result of this calculation is shown in Fig. 12 (curve a). There is no close agreement between curve a and curve c. However, they are comparable in magnitude. Thus, measurement of very slight changes of profile with wavelength, such as are shown in Fig. 12, are of great practical importance.

VI. CONCLUSION AND PROPOSALS FOR FUTURE WORK

We have proposed and demonstrated a novel technique for measurement of the index profile of multimode fibers. Conceptually, this technique is related to the near-field technique previously demonstrated by Sladen et al.[5] (near-field technique). From a practical point of view, however, our technique is quite different, since it does not require Lambertian sources. In particular, lasers can be used. We have found that the measured profiles are highly reproducible, to better than one part in 1000 over periods of hours. Index profile measurements can be obtained in a few minutes including fiber-end preparation. The agreement between our technique and interferometric measurements leaves something to be desired. The discrepancy, however, may be attributed to the lack of perfect circular symmetry of the fibers investigated. Theoretical considerations show that the res-

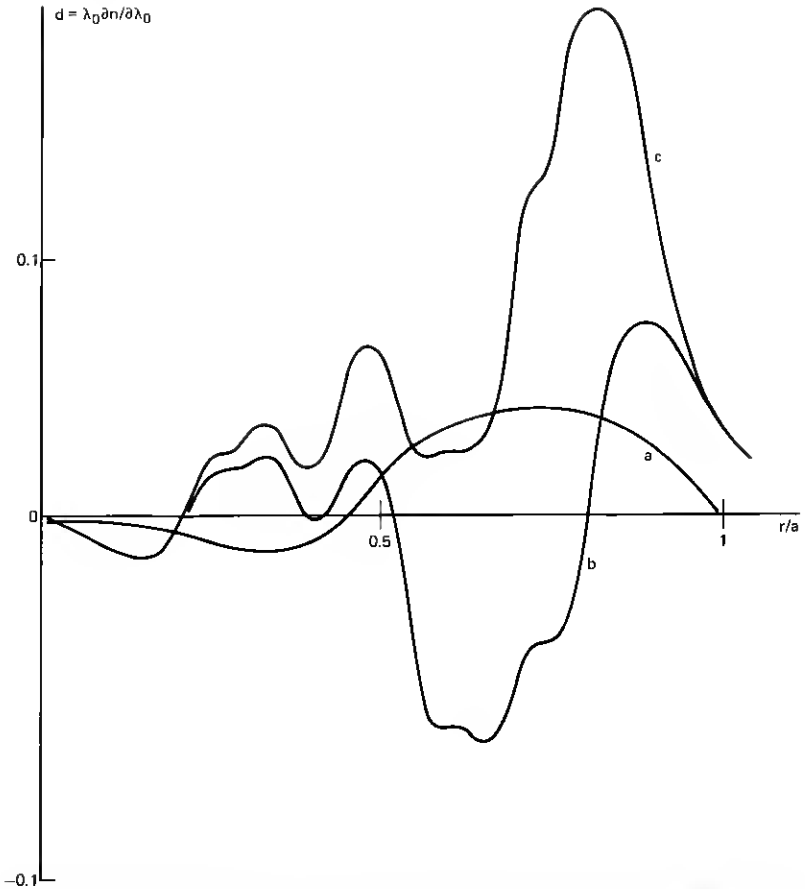

Fig. 12—Profile distortion. Curve (a) is calculated from Fleming's measurements on bulk samples as reported in Ref. 3 (Fig. 1, curve labeled $\lambda = 0.9$ μm). Curve (b) is the difference between the normalized profiles at $\lambda_0 = 0.79$ and 0.9 μm. Curve (c) is the same as curve (b) corrected for the leaky rays.

olution is about $\lambda/4\sqrt{2\Delta}$. For a typical value $\Delta \approx 0.015$, this resolution is about the free-space wavelength $\lambda_o \approx 1$ μm. This appears to be sufficient for most practical purposes.

Comparison of depths of central-index dips suggests that the transmission technique (and the near-field technique as well) provides better resolution than interferometric techniques. We have presented preliminary evidence for the distortion of the index profile as the wavelength varies (profile distortion), an effect that was inferred previously only from measurements on bulk samples. Theories that neglect profile distortion may be in considerable error.

We shall now make a few suggestions for improvement of the

measurement technique. Oil-immersed microscope objectives would he useful to prevent interference effects hetween the ohjective and the fiher tip when monochromatic laser sources are used. The processing of the experimental data can he considerahly improved if the lock-in amplifier and the gauge have digital readouts. The correction factor C, given approximately in Fig. 5, should be recalculated and supplied in digital form. A hetter approach would consist of calculating C from the apparent measured profile and iterating. These iterations, presumahly, can he effected with modest computing time. Noncircularly symmetric profiles can he corrected, in principle, hut the correction prohlem has not heen solved yet. Finally, we attempt to deconvolve the wave-optics effects (discussed in Appendix A) that are most conspicuous in regions where the index varies rapidly. The possihility of performing this deconvolution is intriguing, hut the analytical prohlem remains, to our knowledge, unresolved. The case of fihers with an index harrier hetween the core and the cladding requires further analysis.

Among all the index-profile measurement techniques that have heen proposed so far, the transmission technique that we have described here appears to he the easiest to implement and the most reliahle. Improvement in data processing should make the results quite accurate in most cases.

APPENDIX A

Wave Optics Effects

The result (given in the main text) that the intensity distrihution in the cross section of long multimode fihers is proportional to $k^2(x, y) - k_z^2$, where $k(x, y) \equiv (\omega/c)n(x, y)$ denotes the core wave numher and $k_z \equiv (\omega/c)n_c$ the cladding wave numher, is hased on ray optics (WKB approximation) and on the assumption that rays whose axial wave numher (k_z) is less than k_z are radiating away and do not contrihute to the total intensity. Because the numher of trapped modes carried hy real fihers is finite, the intensity distribution does not follow the fine details of the index profile. This is hecause the optical field cannot vary in transverse directions faster than $(\sin k_{x\,\max}x)$ where $k_{x\,\max} = (\omega/c)n_o\sqrt{2\Delta}$ denotes the maximum value of the transverse wave numher, n_o the index on axis, and $\Delta \approx \Delta n/n$. According to the ahove formula, the smallest distance hetween nodes and peaks of the irradiance in the fiher core is

$$\Delta x \approx \lambda_o/(4n_o\sqrt{2\Delta}). \tag{10}$$

Equation (10) provides an estimate of the resolution afforded hy the

method. For example, if $\lambda_o = 1\ \mu$m, $n_o = 1.45$, and $\Delta = 0.01$, the resolution is, according to (10), $\Delta x \approx 1.25\ \mu$m.

To get a more precise estimate of the error at discontinuities of the index profile, let us consider, as a model, an oversized dielectric slab. When the origin of the x axis is taken at one of the slab boundaries, the normalized field of H-modes of order m is (see, for example, Ref. 6 with a slight change of notation)

$$E_m(x) = \begin{cases} -\frac{1}{\sqrt{2}} \sin\,(Y_m X - \arcsin Y_m), & X \leqq 0, \\ \frac{1}{\sqrt{2}} \exp\,(-\sqrt{1 - Y_m^2} X), & X \geqq 0, \end{cases} \tag{11}$$

where

$$Y_m = (m + 1)(\pi/2) V^{-1} \tag{12}$$

and X, V are normalized distances and frequencies

$$X = k\sqrt{2\Delta}x \tag{13a}$$

$$V = k\sqrt{2\Delta}d. \tag{13b}$$

For trapped modes, we require

$$Y_m < 1. \tag{14}$$

When the fiber is excited by a Lambertian source, the intensity $I(x)$ in the slab cross section is obtained by adding the intensities, $E_m^2(x)$, of all the trapped modes. Because the slab is highly oversized, we can replace the summation over m by an integral. We obtain

$$I(x) = \begin{cases} 2\int_0^{\pi/2} \sin^2\,(\sin\theta X - \theta) \cos\theta d\theta & X \leqq 0 \\ 2\int_0^{\pi/2} \sin^2\theta \exp\,(-2\cos\theta X) \cos\theta d\theta, & X \geqq 0. \end{cases} \tag{15}$$

For $X \to -\infty$ and $X \to +\infty$, we have as expected, $I = 1$ and $I = 0$. At the discontinuity ($X = 0$), an elementary integration of (15) gives $I = \frac{2}{3}$. The intensity profile defined in (15) is shown in Fig. 13. We notice an overshoot of the irradiance equal to 14 percent. This overshoot is somewhat similar to the Gibbs effect encountered with Fourier series. If we keep the slab thickness a constant but increase the optical frequency, the region where the irradiance departs significantly from the ray-optics value becomes narrower and narrower. The amplitude of the overshoot, however, remains the same. The curve in Fig. 13 provides understanding of the limitation in resolution of the method discussed in the main text. This limitation is caused by wave-optics effects that have been ignored in eq. (1).

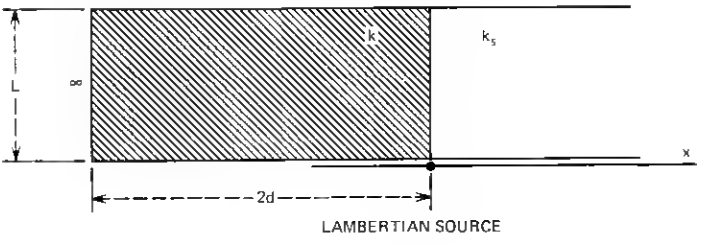

(a)

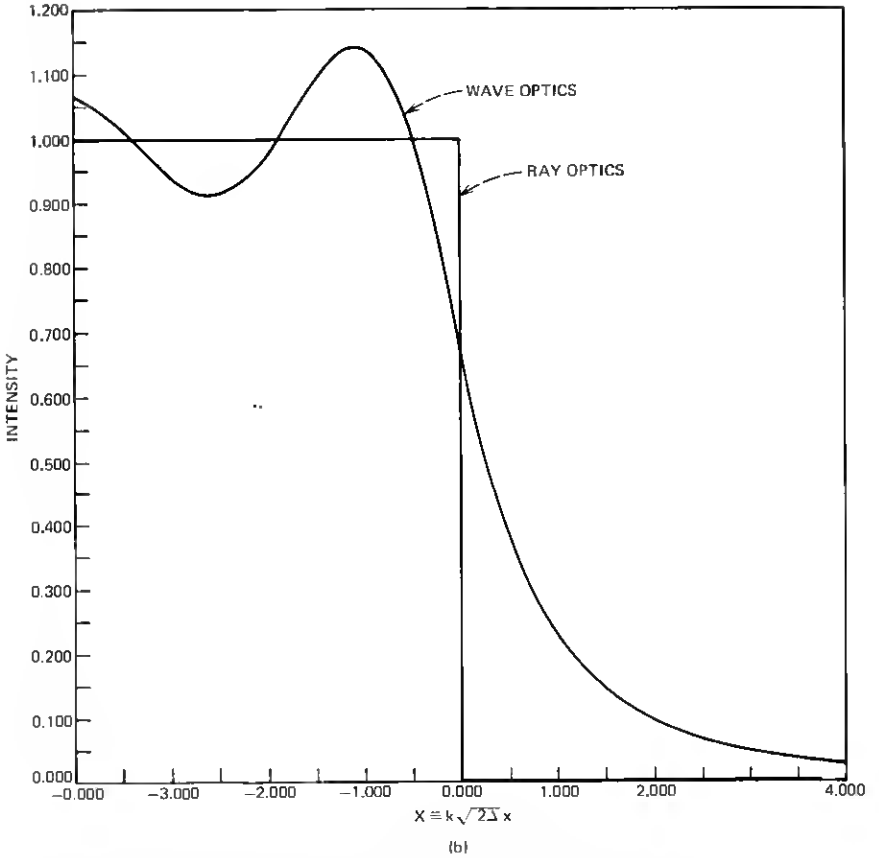

(b)

Fig. 13—Wave-optics effect in highly multimoded slab (a). The curve in (b) exhibits the departure from ray optics. Note the overshoot of 14 percent, which is independent of wavelength.

APPENDIX B

Profile Distortion

In this Appendix we derive formulas relating to the change of shape of the index profile of a fiber as the wavelength varies (independently

of a possible change of scale). These formulas relate the distortions measured directly on the fiber to measurements on bulk samples.

Let us assume that we bave normalized tbe profiles to unity at $r = 0$. Tbe ordinate of the curve is $1 - \eta$, where $\eta = N/2\Delta$, $N(r) \equiv 1 - n^2(r)/n_o^2$ and $2\Delta = 1 - n_c^2/n_o^2$. From the normalized profiles at two closely spaced wavelengths, we evaluate the profile distortion $d(r)$

$$d(r) \equiv \lambda_o \partial\eta/\partial\lambda_o. \tag{16a}$$

This may be written as

$$d = C^{-1}[\lambda_o(\partial P/\partial\lambda_o) + P(X/C)(\partial C/\partial X), \tag{16b}$$

wbere $P(r, \lambda_o)$ is the normalized (but uncorrected) Siber transmission, $C(r, X)$ tbe leaky-ray correction factor, and X is tbe parameter defined in (9).

C and the differential correction term $(X/C)(\partial C/\partial X)$ can be obtained from Fig. 5.

Let us now consider the curve $S(n)$ wbere $S \equiv -\lambda_o n \partial n/\partial\lambda_o$ tbat can be obtained from measurements on hulk samples. From the value of Δ and the cladding index n_c, we calculate the index on axis n_o. It is not difficult to show [e.g., from eq. (14) of Ref. 11] that the distortion parameter d defined in (16) is related to the dispersion parameter S defined above by

$$d(\eta) = [D_o/\Delta(n_o^2 + S_o)][s(\eta) - \eta s(1)], \tag{17}$$

where we have defined

$$D_o \equiv 1 - (\lambda_o/n_o)(\partial n_o/\partial\lambda_o), \tag{18}$$

and

$$s \equiv S(n) - S(n_o) \tag{19}$$

is considered a function of η. In particular, $s(1) \equiv S(n_c) - S(n_o)$. It is clear, from its definition and from (17), that

$$d(0) = d(1) = 0. \tag{20}$$

REFERENCES

1. E. A. J. Marcatili, private communication.
2. J. A. Arnaud, unpublished work.
3. J. A. Arnaud and J. W. Fleming, "Pulse Broadening in Multimode Optical Fibers with Large $\Delta n/n$ Numerical Results," Electron. Lett., *12*, No. 7 (April 1976).
4. D. Gloge and E. A. J. Marcatili, "Multimode Theory of Graded Core Fibers," B.S.T.J., *52* (November 1973), pp. 1563–1578.
5. F. M. E. Sladen, D. N. Payne, and M. J. Adams, "Determination of Optical Fiber Refraction Index Profiles by a Near-Field Scanning Technique," Appl. Phys. Lett., *28*, No. 5 (March 1, 1975), p. 255.
6. J. A. Arnaud, *Beam and Fiber Optics*, New York: Academic Press, 1976.
7. J. Stone and H. E. Earl, "Surface Effects and Reflection Refractometry of Optical Fibers," Opt. Quant. Elec., *8* (1976), pp. 459–463.
8. H. M. Presby, private communication.
9. J. B. MacChesney, private communication.
10. J. B. MacChesney and P. B. O'Connor, private communication.
11. J. A. Arnaud, "Numerical Evaluation of the Impulse Response of Multimode Optical Fibers," unpublished work.